MODELING OF SOLAR AIR-CONDITIONING SYSTEMS USING MODELICA

Miquel Alomar Barceló, Víctor Martínez Moll, Andreu Moià Pol

University of Balearic Islands, Physics department, P. Mallorca (Spain)

1. Abstract

An investigation about the best procedures to increase the solar fraction of the total energy consumption in hotels has been started. Several configurations of solar cooling and heating systems for buildings have been designed to achieve different values of the fraction of primary energy saving using either the solar thermal or the photovoltaic (PV) technology.

The main aim of this paper is to describe the simulation models of different solar air-conditioning systems and their components. The models, developed in the Modelica language, will enable a systematic comparative energy and economical analysis of the use of solar thermal and PV technologies to meet energy demands of a building.

2. Introduction

Air-conditioning (AC) is one of the indispensable provisions in modern life. Normally, one third to half of the annual total electricity consumption is used for air-conditioning and refrigeration in the metropolis worldwide. 80% of electricity is still generated by burning the fossil fuels, leading to non-stopping emission of global warming gases (Fong et al. 2009).

Solar cooling and heating is a sustainable means to provide air-conditioning that has a positive and long-term impact. For the continual population and economic growth, wider use of solar energy in air-conditioning would secure the increasing energy demand for this use.

Recent studies indicate that solar electric compression refrigeration and solar absorption refrigeration are the solar cooling options with the highest energy saving potential (Fong et al. 2009). The former uses the solar electric gain, while the latter uses solar heat.

The option of simple electricity compensation of conventional cooling installations by electricity from grid connected PV panels has its advantages and disadvantages when compared to solar thermal absorption cooling.

The PV approach is very attractive, since electricity feed-in regulations exist in some European countries, which allow not requiring electricity storage. Furthermore, investment costs for the cooling plant are comparatively low, mainly due to the use of conventional cooling technologies. Nevertheless, preliminary calculations (Wiemken et al. 2010) indicate that the real-time coverage of the electricity demand in a PV/conventional system may not always compete with a solar thermally driven system without additional measures. Such a system does not eliminate the dependence on public grid during peak cooling demands in hot summer days. Furthermore, refrigerants with usually high global warming potential are applied.

A systematic comparison of both technologies remains an important task in the near future.

In the first part of this paper (section 3), different schematic diagrams of the solar cooling and heating systems including either PV panels or solar thermal collectors, are presented.

In section 4, the component models developed in the Modelica language are described in detail.

The developed models will enable a comprehensive simulation-based analysis of the use of solar thermal and PV technologies to meet energy demands of a building.

3. Configurations of the solar AC systems

As the feasibility of a solar system depends on its fraction of primary energy saving, different plant configurations, including different elements, are proposed according to the level of solar contribution both for the thermal and PV options.

A low solar fraction thermal system, for example, that only meets the domestic hot water (DHW) energy demand, requires a conventional electric vapor-compression chiller, while a higher solar contribution system which covers completely the DHW demand and partly the heating and cooling loads, includes a greater collector surface area and an absorption chiller instead of the conventional one.

The basic reference system includes the minimum solar collector area to partly meet DHW energy demands of the building, between 30 and 70% depending on the climatic zone and on the building demand, according to the criterion given at the Spanish Energy Saving Basic Document (DB HE).

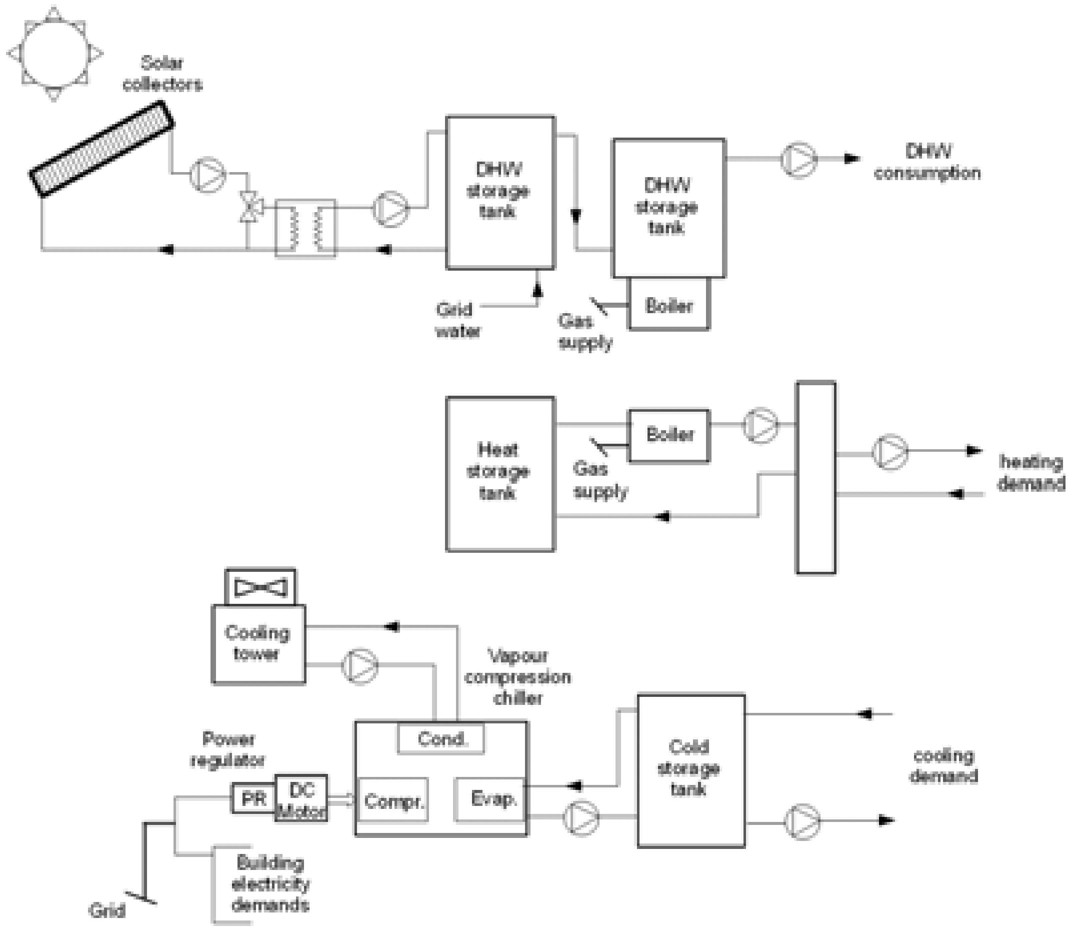

Fig. 1: Schematic diagram of the basic reference system

In the high solar fraction system, DHW tank temperature controls whether the solar energy must contribute to the DHW or to the heating/cooling (winter/summer) production.

Auxiliary boiler set point temperature must be high (about 85 ºC) during summer in order to activate the absorption machine for cooling production, but can be reduced (to about 40 ºC) in winter time if fan coils are used in the heating system.

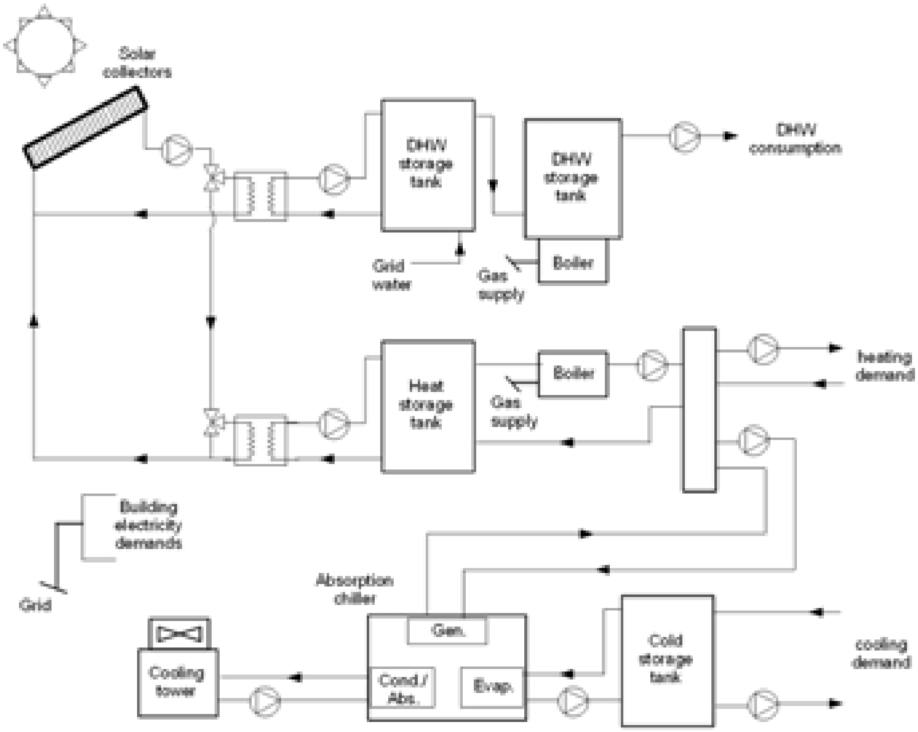

Fig. 2: Schematic diagram of the high solar thermal contribution system

In the PV system case, the PV panels compensate the chiller or building electricity consumptions to a greater or lesser extent depending on the available panel surface. The system also includes the minimum solar thermal collector area required to partly meet DHW energy demands of the building.

Another possibility for the PV system case is to use the electrical heat pump, instead of the gas boiler, for the heating production.

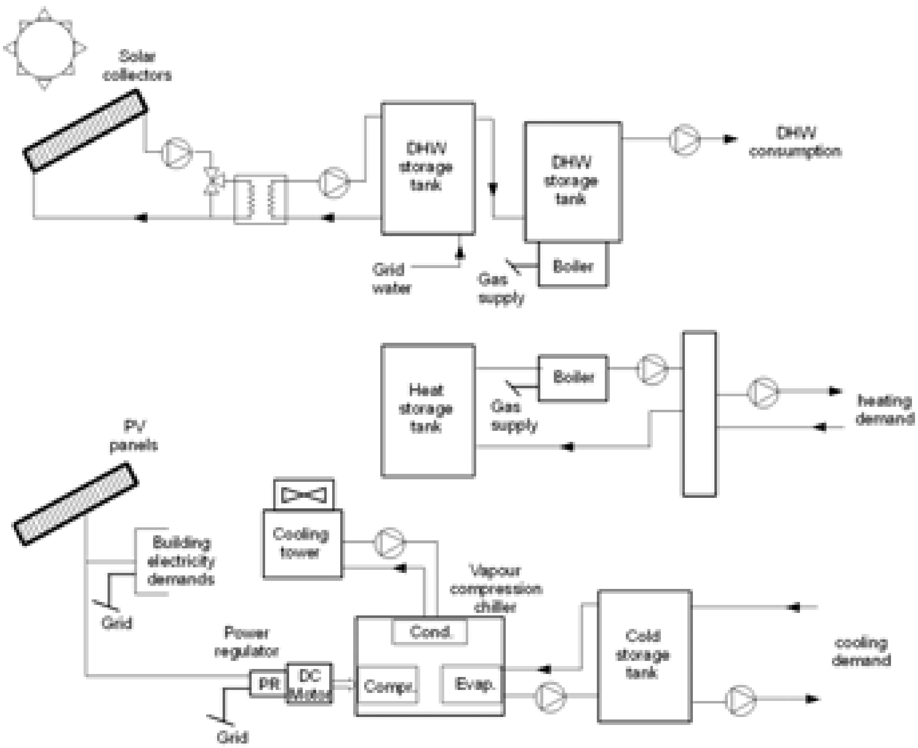

Fig. 3: Schematic diagram of the PV system

4. Component models library

Models of the components of the solar cooling and heating plants have been developed by means of the physical laws that describe the relevant properties with the goal of emulating their thermal and energetic behavior. Models have been developed for the next elements:

- Pipe
- Pump
- Boiler
- Fully mixed thermal storage tank
- Manifold tank
- Stratified thermal storage tank
- Heat exchanger
- Solar thermal collector
- Cooling tower
- Absorption chiller
- Vapor-compression water chiller
- Load emulator
- PV panel
- Weather and solar position data generation

The components modeling has been carried out in the *Modelica* language, which is an open, object-oriented, non calculation-causal (based on equations, no particular variables need to be solved manually) simulation system, which is suited for modeling complex physical systems that consist of interconnected sub-components. The software used for this application was *Dymola/Modelica*, specifically *Dymola 7.0* from *Dynasim*.

Even though solar cooling with thermally driven absorption chillers allows for primary energy savings and reductions in peak load electricity consumption from the grid, most of the current solar absorption cooling installations do not achieve the desired performances to compete with conventional chillers, especially with respect to the auxiliary electricity consumption (Wiemken et al. 2010; Thür et al. 2010). Therefore, it is of great importance a correct component modeling that takes into account electricity consumptions in order to optimize the electrical COP of the systems.

The chosen simulation environment, unlike others like TRNSYS, enables an accurate calculation of the pressure drop on each component and the corresponding pump electricity consumption.

Other advantages, apart from the simplicity of creating new model libraries or modifying the already made ones, are the possibility of using a medium with variable properties (specific heat and density) depending on temperature, using an inertia mass in each desired component or starting simulations at the desired temperature. Below, the developed component models are described in detail.

<u>Pipe</u>

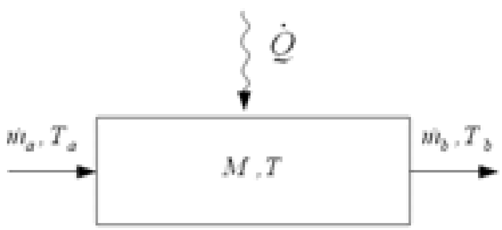

Fig. 4: Schematic diagram of the pipe component

The pipe model is based on the standard 'Thermal.FluidHeatFlow.Components' Modelica library 'HeatedPipe' component. Both heat exchange with the ambient (thermal losses) and fluid friction heat are considered:

$$\dot{Q} = \dot{Q}_{frict} + \dot{Q}_{loss} \quad \text{(eq. 1)}$$

Mass balance is applied:

$$\dot{m}_a = -\dot{m}_b = \dot{m} \quad \text{(eq. 2)}$$

Energy balance is applied to determine temperature evolution of the mass of medium within pipe (M):

$$\dot{H}_a + \dot{H}_b + \dot{Q} = M \cdot c_p \frac{dT}{dt} \quad \text{(eq. 3)}$$

Assuming a positive mass flow from ‘a’ to ‘b’, mixing rule is applied at ‘a’ and energy flow at ‘b’ is defined by medium’s temperature:

$$\dot{H}_a = \dot{m} \cdot h_a \quad \text{(eq. 4)}$$

$$\dot{H}_b = -\dot{m} \cdot h \quad \text{(eq. 5)}$$

Where enthalpies are given by

$$h = c_p \cdot T \; , \; h_a = c_p \cdot T_a \quad \text{(eq. 6)}$$

Thermal losses are calculated from ambient temperature, T_a, overall thermal losses coefficient for each pipe meter, G, and pipe length, L, according to

$$\dot{Q}_{loss} = -G \cdot L \cdot (T - T_a) \quad \text{(eq. 7)}$$

Pressure drop, *dP*, for each meter of pipe is determined assuming a linear dependency of pressure drop on volume flow in the laminar region and a quadratic dependency in the turbulent region, linear and turbulent dependencies are coupled smoothly:

$$dP = \left\{ \begin{array}{l} \alpha \dot{V} \text{, } if \quad \dot{V} \leq \dot{V}_{lam} \\ \alpha \dot{V} + k \cdot (\dot{V} - \dot{V}_{lam})^2 \text{, } if \quad \dot{V} > \dot{V}_{lam} \end{array} \right\} \quad \text{(eq. 8)}$$

Coefficients α and k are calculated by means of two operation points, one in the laminar region and the other in the nominal (turbulent) region, which must be obtained from catalogue data or available measurements:

$$(\dot{V}_{lam}, dP_{lam}) \; , \; (\dot{V}_{nom}, dP_{nom}) \quad \text{(eq. 9)}$$

$$\alpha = \frac{dP_{lam}}{\dot{V}_{lam}} \; , \quad k = \frac{dP_{nom} - \alpha \dot{V}_{nom}}{(\dot{V}_{nom} - \dot{V}_{lam})^2} \quad \text{(eq. 10)}$$

Friction heat rate is given by the product of volume flow rate and total pipe pressure drop:

$$Q_{frict} = \dot{V} \cdot dP \cdot L \quad \text{(eq. 11)}$$

The described approach to calculate pipe's pressure drop has also been used in other components.

Pump

The pump model is based on the standard 'Thermal.FluidHeatFlow.Sources' Modelica library 'VolumeFlow' component. It models a variable speed pump that is able to maintain any desired fraction of the design volume flow rate (given as an input) by speed control with no sacrifice in efficiency, η.

Pressure increase, *dP*, is given by the response of the whole system. Heat exchange with medium is considered. An amount of mass of medium within the pump, at a temperature that evolves according to the mixing rule, is considered.

Hydraulic power is given by

$$\dot{W} = dP \cdot \dot{V} \qquad \text{(eq. 12)}$$

The required electrical input power is calculated as

$$\dot{W}_{elect} = \frac{\dot{W}}{\eta} \qquad \text{(eq. 13)}$$

The energy transferred from the pump to the fluid stream is calculated as

$$\dot{Q} = (\dot{W}_{elect} - \dot{W}) \cdot f \qquad \text{(eq. 14)}$$

Where parameter *f* is defined as the fraction of pump inefficiencies that contribute to a temperature rise in the fluid stream passing through the pump; the remainder of these inefficiencies contribute to an ambient temperature rise.

Boiler

The boiler has been modeled to elevate the temperature of a flow stream, at an input temperature T_i, with a heat rate limited by a maximum and a minimum value. The boiler can modulate its heating capacity to any required load in the allowed range to achieve a desired set point temperature T_{set} :

$$\dot{Q}_{requ} = \dot{m} \cdot c_p \cdot (T_{set} - T_i) \qquad \text{(eq. 15)}$$

Activation/deactivation of the boiler is controlled by a hysteresys cycle depending on boiler's outlet temperature. When the boiler is 'on', its heating power is given by:

$$\dot{Q}_{boiler} = \left\{ \begin{array}{l} \dot{Q}_{max}, \ \mathit{if} \quad \dot{Q}_{req} > \dot{Q}_{max} \\ \dot{Q}_{requ}, \ \mathit{if} \quad \dot{Q}_{min} \leqslant \dot{Q}_{req} \leqslant \dot{Q}_{max} \\ \dot{Q}_{min}, \ \mathit{if} \quad \dot{Q}_{req} < \dot{Q}_{min} \end{array} \right\} \qquad \text{(eq. 16)}$$

A fully mixed storage volume is considered within the boiler. Pressure drop between input and output is calculated according to the same approach used for the pipe model. The primary energy consumption of the boiler can determined from the energy delivered to the flow stream and the energy efficiency for gas energy (or any other) converted into primary energy, η_g :

$$E_{primary} = \frac{Q_{boiler}}{\eta_g} \qquad \text{(eq. 17)}$$

When the boiler is operated by burning gas, η_g is assumed to be approximately 90%.

Fully mixed storage tank

This component models the simplest case of a thermal storage tank: the whole mass of water within the tank, M, is assumed to be fully mixed, at a homogeneous temperature T_1.

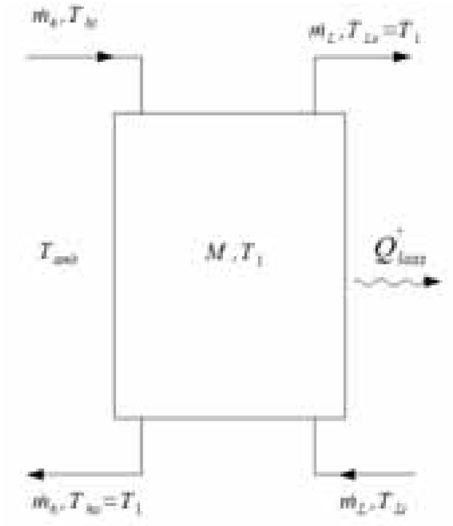

Fig. 5: Schematic diagram of the fully mixed storage tank

The fully mixed tank model is analogous to the pipe model, but four flow ports (heat source input and output from one side, and load input and output from the other side), instead of two, must be considered in this case. The energy balance equation is

$$c_p \cdot \dot{m}_h (T_{hi} - T_{ho}) + c_p \cdot \dot{m}_L (T_{Li} - T_{Lo}) + \dot{Q}_{loss} + \dot{Q}_{frict} = c_p \cdot M \frac{dT_1}{dt} \qquad \text{(eq. 18)}$$

In terms of the enthalpy flow rates, the equation results

$$\dot{H}_{hi} + \dot{H}_{ho} + \dot{H}_{Li} + \dot{H}_{Lo} + \dot{Q}_{loss} + \dot{Q}_{frict} = c_p \cdot M \frac{dT_1}{dt} \qquad \text{(eq. 19)}$$

Where the enthalpy flow rates for each flow port can be expressed analogously as in equations (4) and (5). Pressure drop and the corresponding friction heat term are calculated separately for each circuit (heat source and load) using the same approach as for the pipe model.

Manifold tank

This component is useful to distribute the energy from a heat source circuit to different building loads.

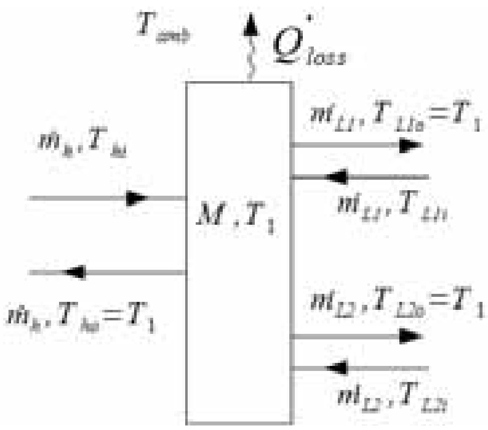

Fig. 6: Schematic diagram of the manifold tank

The storage volume is assumed to be fully mixed, therefore the model equations are analogous to the fully mixed tank model, but additional flow ports for the additional load circuit must be considered:

$$\dot{H}_{hi} + \dot{H}_{ho} + \dot{H}_{L1i} + \dot{H}_{L1o} + \dot{H}_{L2i} + \dot{H}_{L2o} + \dot{Q}_{loss} + \dot{Q}_{frict} = c_p \cdot M \frac{dT_1}{dt} \qquad \text{(eq. 20)}$$

Pressure drop and the corresponding friction heat term are calculated separately for each circuit using the same approach as for the pipe model.

<u>Stratified storage tank</u>

The 'multinode' approach (Kleinbach et al., 1993; Duffie and Beckmann, 1991) has been used to model a stratified thermal storage tank with fixed inlet positions. In this approach, the tank is modeled as N fully mixed volume segments (nodes) with an energy balance for each node. It results in a set of N differential equations that can be solved for the temperatures of the nodes as a function of time.

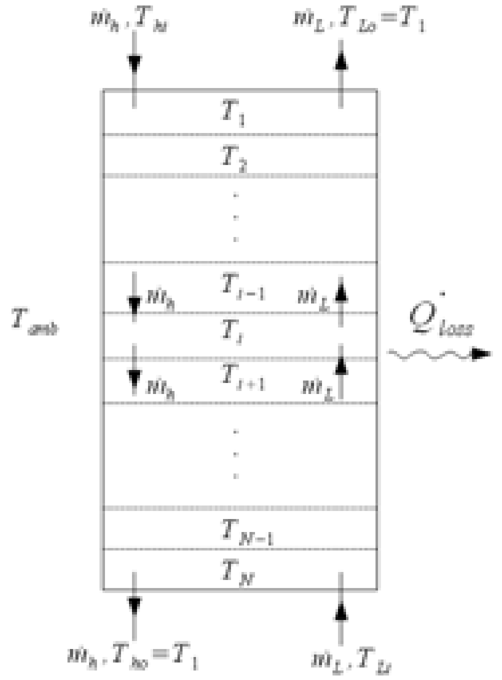

Fig. 7: Schematic diagram of the stratified storage tank

The degree of stratification is determined by the choice of N. This method assumes that the major cause of stratification is the mixing introduced during charge and discharge cycles. The inlet and outlet positions of the fluids from heat source and load can be chosen (usually at the top and bottom of the tank).

At the end of each time step, any temperature inversions that result from these flows are eliminated by mixing appropriate nodes. This mixture process models the reduction of stratification, induced by convective currents, in the case that the temperature of the heat source incoming fluid is cooler than the upper portion of the tank.

An assumption used in the model is that the fluid streams flowing up and down from each node are mixed before they enter each node, and a resultant flow, either up or down, is determined before an energy balance on the nodes is done. Pressure drop between input and output both for the heat source and load circuits, as well as the corresponding friction heat terms, have been included following the same approach used for the pipe model.

In order to check the correct implementation of the stratified storage tank model in the Modelica language, an exemplary system has been simulated using *Dymola/Modelica* and *TRNSYS* software. The system consists of a 5-nodes storage tank with the heat source inlet and outlet positions at nodes 2 and 5, respectively, and at nodes 5 and 1 for the load circuit. Heat source mass flow rate takes a constant value of 7920 kg/h, but inlet temperature evolves according to

$$T_{hi} = 80 + 8 \cdot \sin\left(\frac{1}{2} \cdot 2\pi t\right) \cdot \exp\left(-\frac{1}{3} t\right) \qquad \text{(eq. 21)}$$

Where temperature is given in ºC and time, t, in hours. Load flow stream enters at constant mass flow rate of 2160 kg/h, and constant temperature of 15 ºC. Initial tank temperature is 0 ºC, the tank volume is 3 m^3 and overall heat loss coefficient is 1.25 kJ/(h·m^2·K). Friction heat terms have been neglected.

The results obtained with both simulation programs showed good agreement for the tank temperature distribution and for the heat rates entering and leaving the tank. It can be seen that temperature inversions do not take place in the tank. As time goes on and the temperature distribution becomes stationary, input and output tank powers tend to equal each other showing that energy is conserved.

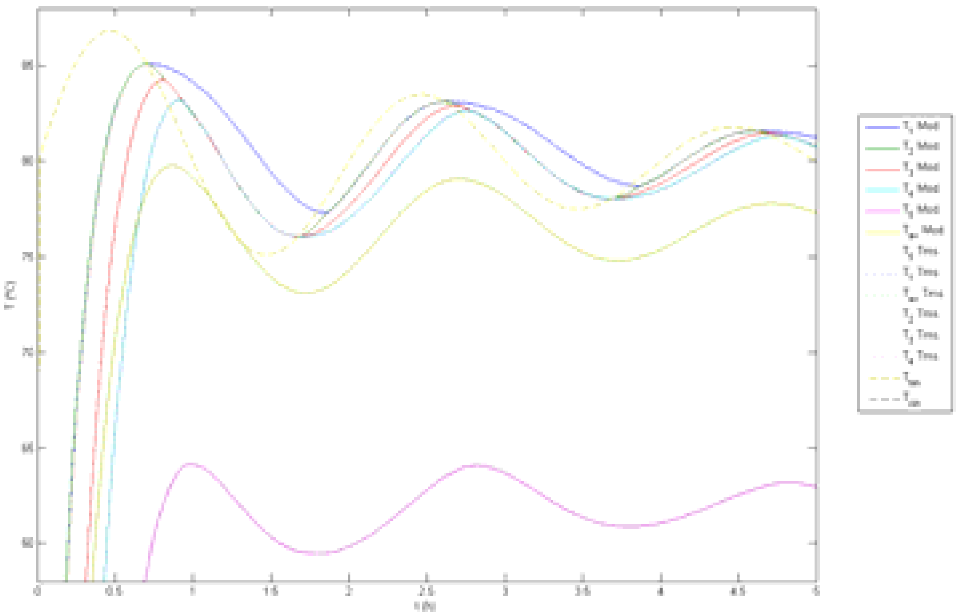

Fig. 8: Evolution of a 5-node stratified storage tank temperatures. Dotted lines show TRNSYS results and continuous lines show Modelica/Dymola results.

Heat exchanger, solar thermal collector and cooling tower

The heat exchanger, solar thermal collector (with biaxial Incidence Angle Modifiers) and cooling tower models have been based on TRNSYS 16 types 5, 71 and 51, respectively, whose mathematical description is covered in the TRNSYS manual.

Pressure drop at these components has been calculated according to the same approach used for the pipe model. An amount of inertia mass of medium within these components, at a homogeneous temperature that evolves according to the mixing rule, has also been considered.

The correct implementation of these models in the Modelica language has been verified with TRNSYS simulations of exemplary systems including the components.

Absorption chiller

The complete thermodynamic models of thermal chillers include many equations with a non-linear structure that has hindered the development of reliable programmed solver modules of absorption machines for simulating performance in detailed energy optimization programs. On the other hand, knowledge of specific design parameters of each machine, normally not provided by manufacturers, is required to use this kind of extensive numerical models of the internal thermodynamic cycle.

In this work, the model presented by Kühn and Ziegler (2005) has been used. It is an adaptation of the characteristic equation method (Hellmann et al., 1999) that can be used to fit catalogue or experimental data of single- and double-effect absorption chillers to reduce their operating characteristics into easier to handle simple algebraic equations. With this approach, both the cooling capacity and the COP of the chiller are expressed as functions of the external heat exchanger fluid temperatures combined in the so-called characteristic temperature difference (ΔΔt'):

$$\Delta\Delta t' = t_G - a \cdot t_{AC} + e \cdot t_E \quad \text{(eq. 22)}$$

Where t_G, t_{AC} and t_E are the external arithmetic mean temperatures of generator, absorber-condenser and evaporator. Cooling capacity is given by

$$Q_E = s' \cdot \Delta\Delta t' + r \quad \text{(eq. 23)}$$

Insertion of ΔΔt' in the characteristic equation yields

$$Q_E = s' \cdot t_G + s' \cdot a \cdot t_{AC} + s' \cdot e \cdot t_E + r \quad \text{(eq. 24)}$$

The required energy input to the generator can also be expressed as

$$Q_G = s_2' \cdot \Delta\Delta t' + r_2 \quad \text{(eq. 25)}$$

These equations can be used to determine cooling and heat driving capacity depending on external temperatures when the chiller is 'on'. An amount of inertia mass of water is considered within each heat exchanger (generator, absorber-condenser and evaporator). Heat exchange at the condenser and thermal COP are determined by

$$Q_{AC} = -(Q_E + Q_G) \quad \text{(eq. 26)}$$

$$COP = \frac{Q_E}{Q_G} \quad \text{(eq. 27)}$$

Pressure drop at each heat exchanger is calculated according to the same approach used for the pipe model.

Kühn and Ziegler approach has been used by Puig-Arnavat et al. (2010) to fit catalogue and experimental data from several single and double-effect absorption chillers with good results: in general, the data points were in the 10% deviation range, and the obtained r-squared coefficients for ΔΔt' were above 0.9454.

This approach can be used to describe the behavior of a chiller at design flow rates and different external temperatures with a simple linear equation. For this model, the cooling capacity can be modulated varying operation external temperatures, but not flow rates.

Vapor-compression water chiller

The main components of a vapor-compression water chiller include compressor and its driver, condenser, throttling device, and evaporator (liquid cooler). The coefficient of performance (COP) for water chillers is defined as the ratio of the evaporator cooling capacity to the compressor input power:

$$COP = \frac{Q_e}{W_c} \quad \text{(eq. 28)}$$

For the purpose of performance prediction, it is more convenient to express chiller performance COP in terms of readily measured water-side data rather than refrigerant-side data. There are different models (Lee and Lu, 2010) to predict chiller performance COP in terms of readily measured water-side data (condenser inlet and outlet water temperatures, evaporator inlet and outlet water temperatures, and condenser and evaporator water flow rates).

Gordon-Ng empirically-based model (Gordon and Ng, 2000) have been used in this work. This is a gray-box model, its functional form allows the parameter estimates be traced to actual physical principles that govern the performance of the water chillers being modeled. Model parameters or fitting coefficients are determined using a regression method applied to a set of training data. The Gordon-Ng model correlates the chiller COP (dependent variable) with three input independent variables (the water inlet temperature to condenser, water inlet temperature to evaporator, and the cooling capacity of evaporator) according to the following form:

$$\frac{T_{wi}}{T_{ci}}\left(1+\frac{1}{COP}\right)-1=\beta_1\frac{T_{wi}}{Q_e}+\beta_2\frac{T_{ci}-T_{wi}}{T_{ci}Q_e}+\beta_3\frac{Q_e}{T_{ci}}\left(1+\frac{1}{COP}\right) \quad \text{(eq. 29)}$$

A comparative study (Lee and Lu, 2010) that evaluated the suitability of empirically-based performance models for water chillers available in the literature with rich chiller data sets showed that the Gordon-Ng model had acceptable ranges of the overall indicator of model accuracy for all kinds of data sets.

To implement the chiller model, it has been assumed that the chiller can modulate its cooling capacity to any required load in the range between a minimum and maximum value.

Activation/deactivation of the chiller is controlled by a hysteresys cycle depending on water outlet temperature from evaporator. When the chiller is 'on', its cooling capacity is determined by the required power to cool the water to the desired set point temperature, T_{set} (as long as this value is in the allowed range):

$$Q_{requ}=m_e\cdot c_{pe}\cdot(T_{wi}-T_{set}) \quad \text{(eq. 30)}$$

An amount of inertia mass of water is considered both within the evaporator and the condenser. Heat exchange at the condenser is determined by

$$Q_c=|Q_e|+W_c \quad \text{(eq. 31)}$$

Where electricity input power is calculated from equations (27) and (28) given the chiller temperature conditions and loading fraction.

Pressure drop at evaporator and condenser is calculated according to the same approach used for the pipe model.

Load emulator

Three component models have been developed to emulate DHW, heating and cooling building loads. The hourly load profiles must be entered as inputs in a table and they are periodically repeated, every 24 hours, during one month.

The models simply consist of a pump that varies its mass flow rate and the return temperature in order to emulate the desired heating or cooling load:

$$m=Q_{load}/(c_p\cdot\Delta T_{load}) \quad \text{(eq. 32)}$$

In the case of DHW load emulation, the load input and return temperature are given by storage tank top temperature and mains water temperature, respectively; but in the case of heating and cooling loads, the temperature decrease or increase is set as a parameter (usually about 5 K).

PV panel and weather and solar position data generation

These two components have not been developed yet. The Photovoltaic panel is planned to be based on TRNSYS 16 type 94.

Another component must be developed in order to generate year-round weather data at each time step (ambient temperature, relative humidity, overall, beam and diffuse radiation on a chosen surface), as well as the incidence angle for beam radiation and incidence angles in the longitudinal and transversal directions for a surface with a desired orientation; using as input a Typical Meteorological Year (TMY) file.

5. References

Documento Básico HE. Ahorro de energía, 2009. Código Técnico de la Edificación CTE.

Duffie, J. A., and Beckman, W. A., 1991. Solar engineering of thermal processes, 2nd ed., Wiley Interscience, New York.

Dymola, 2011. Demo version of the software available online at www.dynasim.se (Last accessed: July 2011).

Fong, K.F., Chow, T.T., Lee, C.K., Lin, Z., Chan, L.S., 2010. Comparative study of different solar cooling systems for buildings in subtropical city. Solar Energy 84, 227-244.

Gordon, J.M., Ng, K.C., 2000. Cool thermodynamics. Cambridge (UK): Cambridge International Science Publishing.

Hellmann, H.M., Schweigler, C., Ziegler, F., 1999. The characteristic equations of absorption chillers. In: Proc. of the Int. Sorption Heat pump Conf., Munich, pp.169-172.

Kleinbach, E.M., Beckman W.A. and Klein, 1993. Performance study of one-dimensional models for stratified thermal storage tanks, Solar Energy Vol. 50, No 2, pp. 155-166.

Kühn, A., Ziegler, F., 2005. Operational results of a 10 kW absorption chillers and adaptation of the characteristic equation. In: Proc. First Int. Conference Solar Air Conditioning, Bad-Staffelstein.

Lee, T.S., Lu, W.C., 2010. An evaluation of empirically-based models for predicting energy performance of vapor-compression water chillers. Applied Energy 87, 3486-3493.

Modelica, 2011. Modelica standard library available online at www.modelica.org (Last accessed: July 2011).

Puig-Arnavat, M., López-Villada, J., Bruno, J.C., Coronas, A.., 2010. Analysis and parameter identification for characteristic equations of single- and double-effect absorption chillers by means of multivariable regression. International Journal of Refrigeration 33, 70-78.

Thür A., Jähnig D., Núñez, T., Wiemken E., Helm M., Mugnier D., Finocchiaro P., Nocke B., 2010. Monitoring program of small-scale solar heating and cooling systems within IEA-SHC Task 38 – Procedure and first results. Proceedings of the EuroSun 2010, Graz, Austria.

TRNSYS 16, a Transient system simulation program, the solar energy laboratory, University of Wisconsin-Madison, 2006.

Wiemken, E., Wewior, J.W., Elias, A.P., Nienborg, B., Koch, L., 2010. Performance and perspectives of solar cooling. Proceedings of the EuroSun 2010, Graz, Austria.